JOURNAL OF MATERIALS SCIENCE 20 (1985) 3409 – 3417

Creep properties of sintered copper steel

B. COTTERELL, Y. CHOTCHOV, Y. W. MAI
Department of Mechanical Engineering University of Sydney, Sydney, New South Wales 2006, Australia

The creep properties of sintered steel can be described by the normal creep laws. In particular, the activation energy for creep can apparently be identified with that for self diffusion even at temperatures far below $0.5\,T_m$. As might be expected the creep rupture strength of sintered steel is only a small percentage of its ultimate tensile strength. The creep rupture strength depends largely on the ductility and hence better strengths can be expected from alloys with larger ductilities.

Nomenclature

A, B, C, D, E, F	curve fitting parameters	t	time
ΔH_c	creep activation energy	t_R	rupture time
ΔH_d	self diffusion activation energy	y	surface oxide layer thickness
$Q(\sigma)$	stress dependent activation energy	α, β, γ	curve fitting parameters
R	universal gas constant	ε	creep strain
T	absolute temperature	$\varepsilon_0, \varepsilon_1$	strains as defined in Fig. 2
T_m	absolute melting temperature	ε_R	rupture strain
n	creep power law exponent	$\dot{\varepsilon}_s$	secondary creep rate
		σ	applied stress
		σ_R	rupture strength
		σ_0	unit time rupture strength

1. Introduction

Sintered metals are finding increasing use as load bearing components in many areas. Considerable attention has been paid to their fatigue and fracture properties at room tempeature. However, although the properties of sintered and forged superalloys for operation at temperatures of 800° C and above have been studied, the high temperature properties of the more usual sintered alloys have received little attention. Conventional carbon steels can be used satisfactorily up to a temperature of about 500° C. Sintered components might be useful in some applications at these more moderate temperatures. Here we examine the creep properties of a copper steel.

2. Experimental details

Tensile creep tests were performed on specimens (Fig. 1) which were loaded on their wedge-like ends with spit collets. The stress concentration at the end of the test section was minimized by blending the ends with a generous radius. Unfortunately, only some 20% of the specimens failed near the centre of the test section, hence most results are somewhat conservative.

The specimens were compacted from Höganas atomet 28 iron powder with a nominal composition of 0.8% carbon and 2% copper using a pressure of 650 MPa. After sintering the density of the specimens was $6800\,kg\,m^{-3}$. The sintering was performed in two batches which resulted in the final specimens having slightly differing carbon contents. The room temperature tensile properties of the two batches of specimens are given in Table I.

3. Results and discussion

3.1. Tensile creep

A typical creep curve for the sintered steel is

0022–2461/85 $03.00 + .12

TABLE I Room temperature tensile properties

Specimen Batch	Carbon (%)	Average Elongation over 25 mm (%)	Average ultimate tensile strength at room temperature (MPa)		
			As-sintered	Soaked at	
				350° C (30 days)	450° C (32 days)
B	0.89	1.0	470	–	–
C	0.77	1.0	405	388	382

shown in Fig. 2. In common with cast metals there is no tertiary creep stage. The primary creep can be described by the same power law (see Fig. 3)

$$\varepsilon = \varepsilon_0 + \alpha t^n \quad (1)$$

that is often used for conventional metals in the temperature range 0.2 to $0.7\,T_m$ [1]. During secondary creep the strain increases linearly with time.

The dependence of the secondary creep rate $\dot{\varepsilon}_s$ on stress is best described by the exponential law

$$\dot{\varepsilon}_s = A \exp(\beta\sigma) \quad (2)$$

as the plot of $\ln \dot{\varepsilon}_s$ against σ demonstrates (see Fig. 4). The exponential coefficient β does not vary very much over the temperature range 623–723 K. For conventional metals Equation 2 usually only applies for high stress levels, but apparently it applies at even low stress for sintered steels, perhaps because the actual microstresses around the pores must always be high because of the stress concentration caused by them.

For high temperature creep above $0.5\,T_m$, the temperature dependence of the creep rate is usually expressed in terms of a creep activation energy ΔH_c [1], so that with an exponential dependence on stress we have:

$$\dot{\varepsilon}_s = B \exp(\beta\sigma) \exp - (\Delta H_c/RT) \quad (3)$$

High temperature creep is diffusion-controlled and ΔH_c is nearly equal to the activation energy for self diffusion ΔH_d which for a 0.75% carbon steel is 54 kcal mol^{-1} [2]. In Fig. 5 we plot $\ln \dot{\varepsilon}_s$ against $1/T$ for a stress of 220 MPa for Batch B and 350 MPa for Batch C. For Batch C specimens we have one result from a test at 523 K and the resulting plot is remarkably linear. From the slopes of the lines in Fig. 5 we calculate that the activation energies for creep are 52 kcal mol^{-1} for Batch B and 55 kcal mol^{-1} for Batch C specimens. These activation energies are remarkably close to that of self diffusion although the temperatures were well below $0.5\,T_m$ (890 K). Presumably, the pores in sintered metals provide excellent sources or sinks for vacancies and may account for the equality of the activation energies at lower temperatures than is observed with conventional metals.

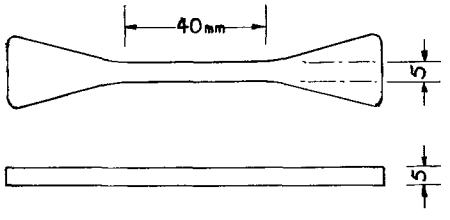

Figure 1 Specimen dimensions in mm.

3.2. Creep rupture

The creep-rupture strengths of the two batches of sintered steel are shown in Fig. 6. Over the range of stress and temperature tested the rupture strength (σ_R) can be related to the rupture time (t_R) by the equation:

$$\sigma_R = \sigma_0 - C \log t_R \quad (4)$$

Apart from a few cleavage facets, the fracture surfaces of room temperature tensile specimens and creep specimens are similar, both showing ductile dimpling (Figs. 7 and 8). Hence we can assume that the creep fracture process is very similar to tensile fracture in these sintered steels and that both occur by coalescence of pores. Not surprisingly the creep-rupture strains (Fig. 9) are similar to the tensile elongations (Table I) and though there is a large scatter do not seem to be greatly affected by the stress level.

In view of the very good correlation of the steady state creep rate with the activation energy it is not surprising that the Orr–Sherby–Dorn (OSD) temperature-compensated time parameter [3] can be used to produce a master creep-rupture curve for sintered steel. It has been

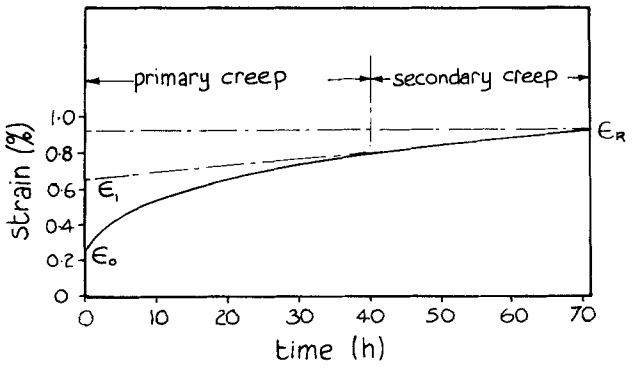

Figure 2 Typical creep curve. Batch C, 623 K. σ = 236 MPa.

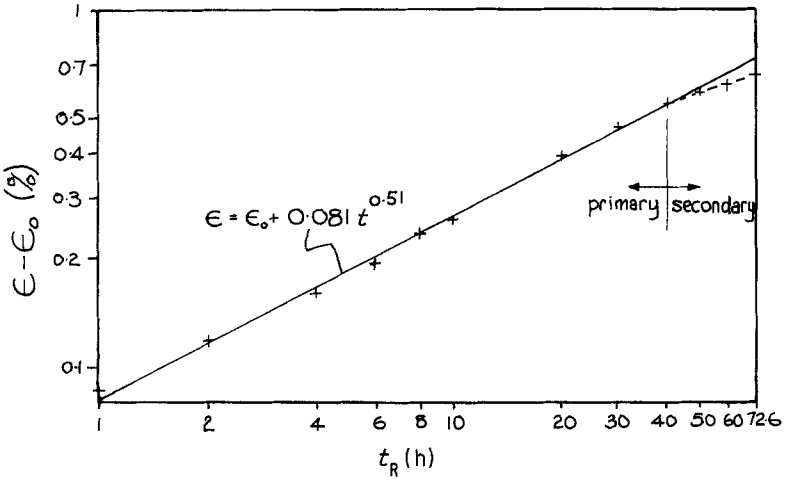

Figure 3 Logarithmic plot of creep curve. Batch C, 623 K. σ = 236 MPa.

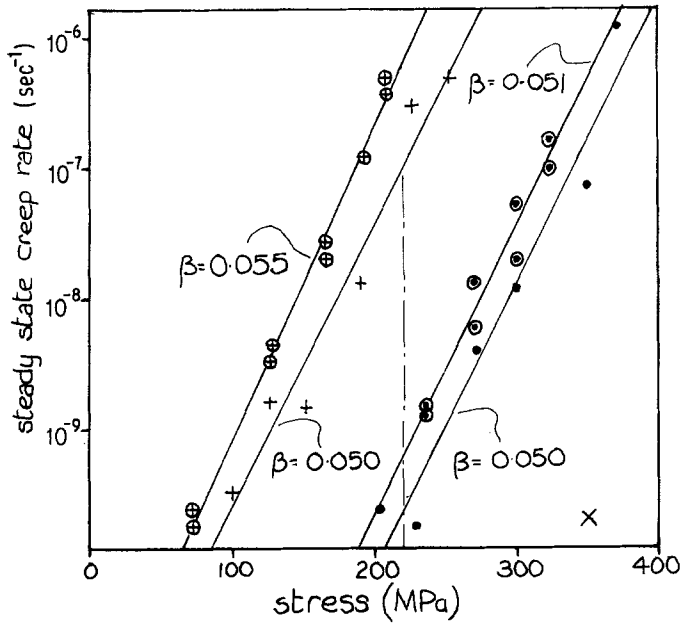

Figure 4 Steady state creep rate as a function of stress. Batch:Temperature (K), ● B:623, + B:723, × C:523, ⊙ C:623. ⊕ C:723.

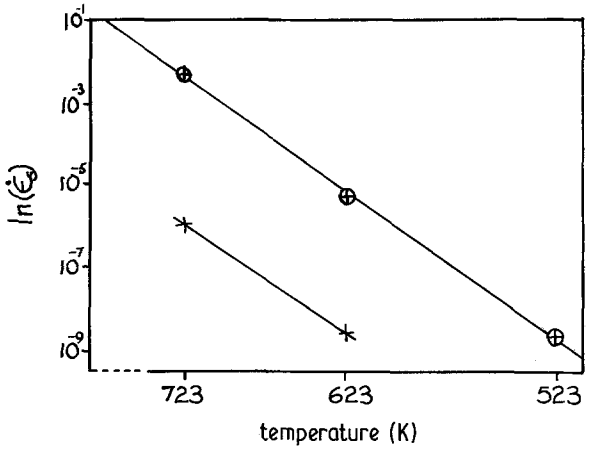

Figure 5 Steady state creep rate as a function of temperature. Batch, + B, ⊕ C.

observed that the creep-rupture time t_R of many metals is inversely proportional to the steady state creep rate $\dot{\varepsilon}_s$ [4, 5] which implies that the strain $(\varepsilon_R - \varepsilon_1)$ shown in Fig. 2 is independent of stress and temperature. Such an assumption seems attractive for sintered metals because we have argued that fracture occurs simply by the coalescence of pores. Hence the rupture time is given from Equation 3 as:

$$t_R = D \exp\left(\frac{\Delta H_c}{RT} - \beta\sigma_R\right) \quad (5)$$

and the rupture stress is given by

$$\sigma_R = \frac{\ln D}{\beta} - \frac{1}{\beta}\left(\ln t_R - \frac{\Delta H_c}{RT}\right) \quad (6)$$

where the term in brackets is the logarithm of the OSD parameter. While the OSD parameter has been useful for correlating creep-rupture data for pure metals and dilute solution alloys, it has not found general acceptance. However, as Fig. 10 shows, this parameter gives excellent correlation for the present data on sintered steel

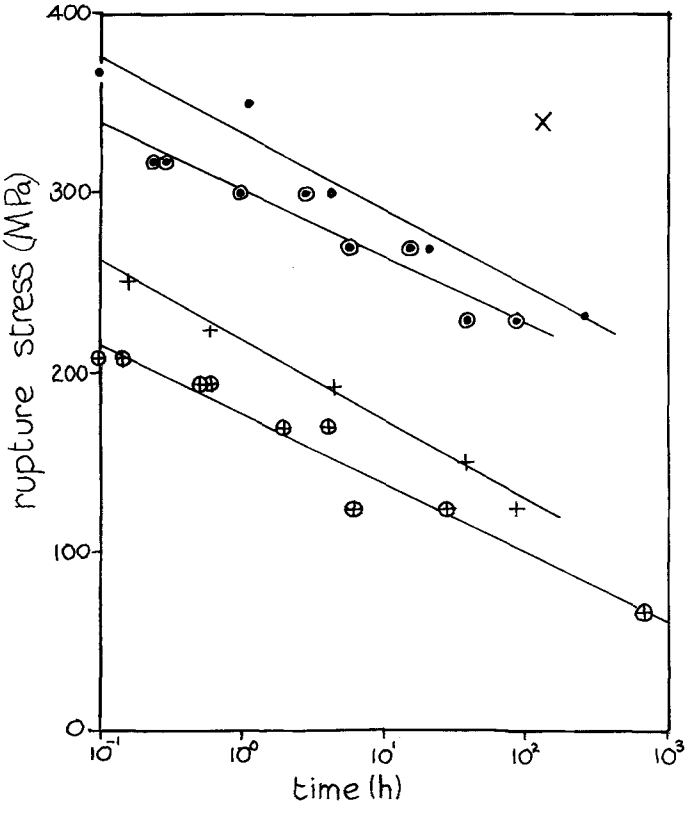

Figure 6 Creep-rupture curves. Batch: Temperature (K), ● B:623, + B:723, × C:523, ⊙ C:623, ⊕ C:723.

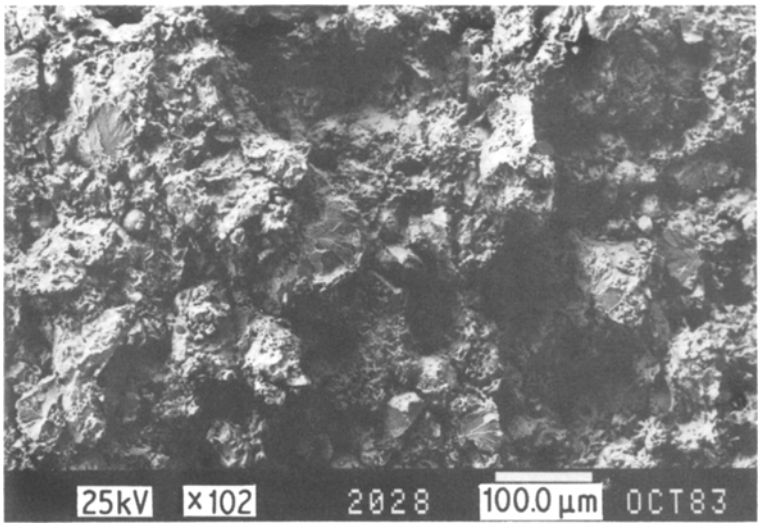

Figure 7 Fracture surface of room temperature tensile test.

which furthermore is linear as predicted by Equation 6. The slopes of the straight line relationships in Fig. 10 are -19.9 and -18.3 for Batches B and C respectively, which are almost precisely the average value of $-1/\beta$ (-19.9 and -18.8) obtained from Fig. 4.

The more usual Larson–Miller parametric method (LM) [6] for creep-rupture data derives from the assumption that the steady-state creep rate is given by

$$\dot{\varepsilon}_s = E \exp -\frac{Q(\sigma)}{RT} \tag{7}$$

where the activation energy Q is dependent on the stress. The creep-rupture time is still assumed to be inversely proportional to the steady-state creep rate so that

$$t_R = F \exp \frac{Q(\sigma)}{RT} \tag{8}$$

and hence

$$\sigma_R = f[T(\log t_R + C)]. \tag{9}$$

Larson and Miller [6] found that for a large range of metals the constant C was approximately 20. Over the range of the present data, Fig. 11 shows that the rupture stress is a linear function of the LM parameter using the original constant of 20. There is no significant difference in the correlation coefficients for the rupture stress as a function of OSD parameter (average 0.991) and the LM parameter (average 0.992) so

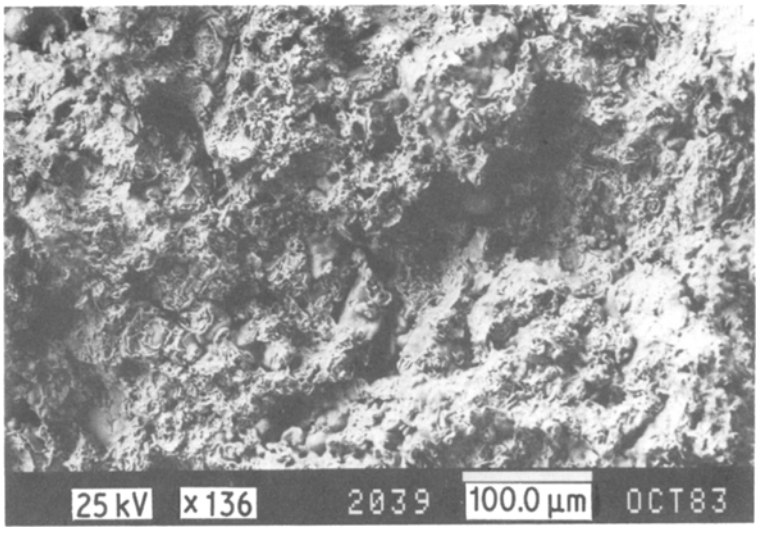

Figure 8 Fracture surface of creep-rupture test at 450° C.

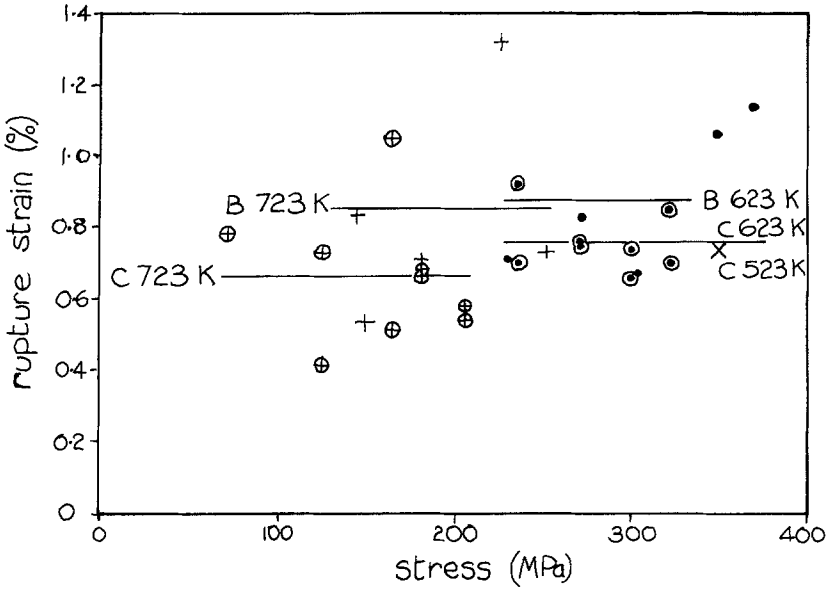

Figure 9 Creep-rupture strain. Batch:Temperature (K), ● B:623, + B:723, × C:523, ○ C:623, ⊕ C:723.

that no statistical distinction can be made between the two parameters. However, because the activation energy for creep estimated from Equation 3 agrees so closely with the activiation energy for self diffusion of iron and because the slope of the rupture stress line in Fig. 10 is so accurately predicted from the steady-state creep data, we believe that the OSD parameter seems preferable. More data over a wider range are, of course, necessary to be more conclusive.

3.3. Effect of oxidation on strength

Because of the porosity, sintered steels oxidize more rapidly than conventional steels so that after 28 days at 450° C the oxide on the surface of a sintered steel specimen is about two and a half times thicker than that on a conventional steel specimen of similar composition. The development in thickness y of the surface oxide layer on a sintered specimen heated to 450° C is shown by a logarithmic plot in Fig. 12. Since

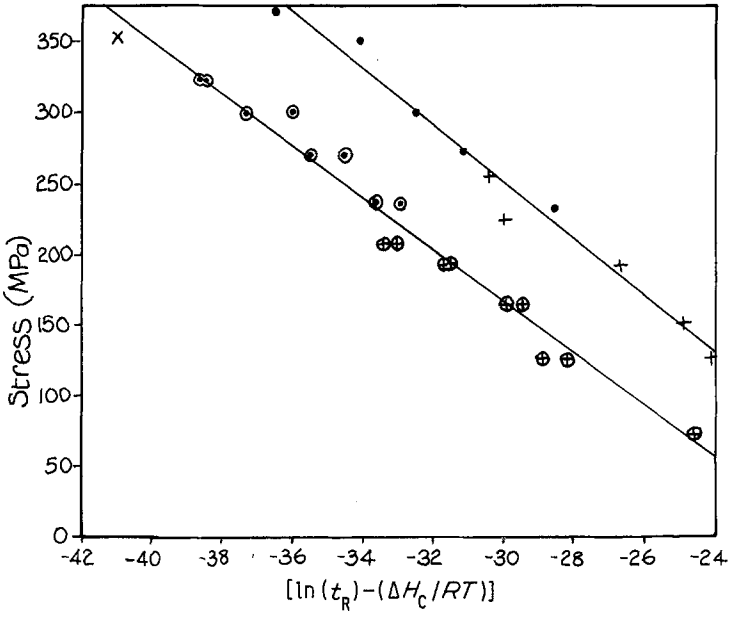

Figure 10 Creep-rupture stress as a function of $[\ln(t_R) - (\Delta H_c/RT)]$.

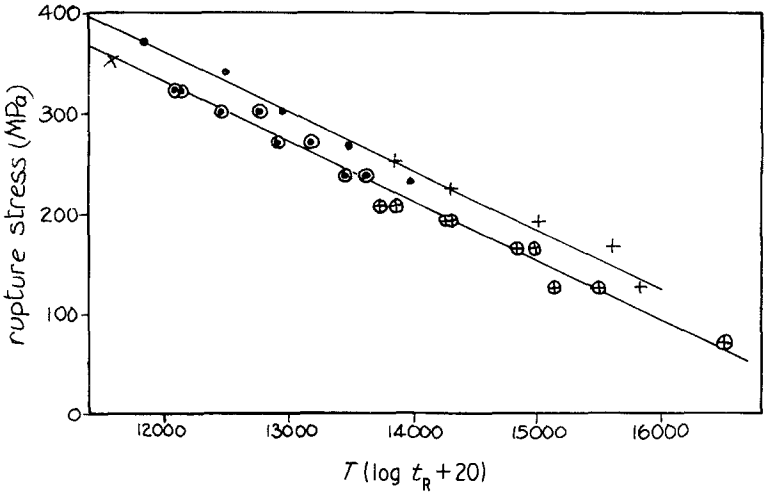

Figure 11 Larson–Miller parametric plot of creep-rupture stress. Batch:Temperature (K), ● B:623, + B:723, × C:523, ⊙ C:623, ⊕ C:723.

there is a linear relationship the growth in thickness can be expressed by a power law

$$y = \gamma t^{0.39} \quad (10)$$

Although the thickness of the surface oxide continues to increase with time, the oxide layers on the internal pores do not grow much thicker than 0.5 μm (Fig. 13). The percentage porosity of the specimens (12.8%) is sufficient to ensure that a large percentage of the pores are interconnected. However, oxidation within the pores will block them and the open porosity decreases preventing further ingress of air – internal oxidation therefore ceases. A similar phenomenon has been observed in steam treatment of sintered steel to improve corrosion resistance [7].

A slight decrease in ultimate tensile strength is shown in specimens that have had prior soaking at elevated temperature (Table I) amounting to about 5.7% for soaking at 450° C. This decrease in strength is due to loss in cross-sectional area due to oxidation. Specimens soaked at 450° C for 32 days gained 3.3% in weight. Since the predominant oxide formed below 506° C is magnetite (Fe_3O_4) [8], for every gram of oxygen gained 2.62 g of iron go into the oxide layer. The percentage decrease in cross-sectional area will be approximately two-thirds of the percentage loss in the volume of iron. Hence the load bearing cross-sectional area of the soaked specimen would have decreased by about $\frac{2}{3} \times 2.62 \times 3.3 = 5.8\%$. Such a decrese in area would lead to the loss in strength observed.

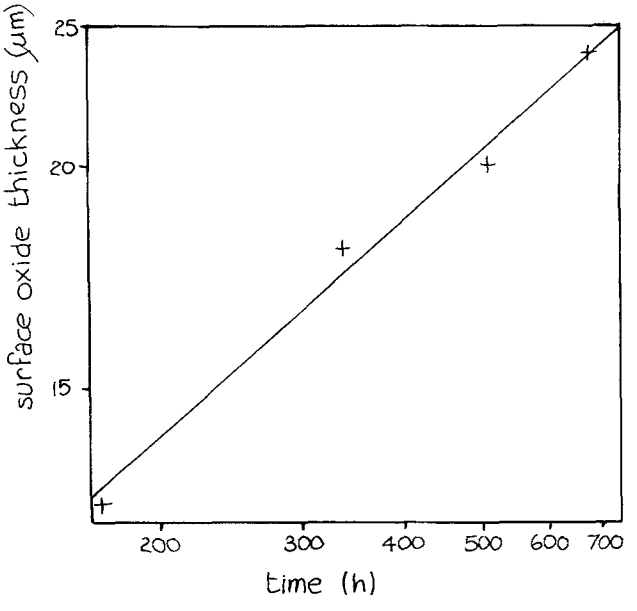

Figure 12 Growth in surface oxide layer. (—)$y = \gamma t^{0.39}$.

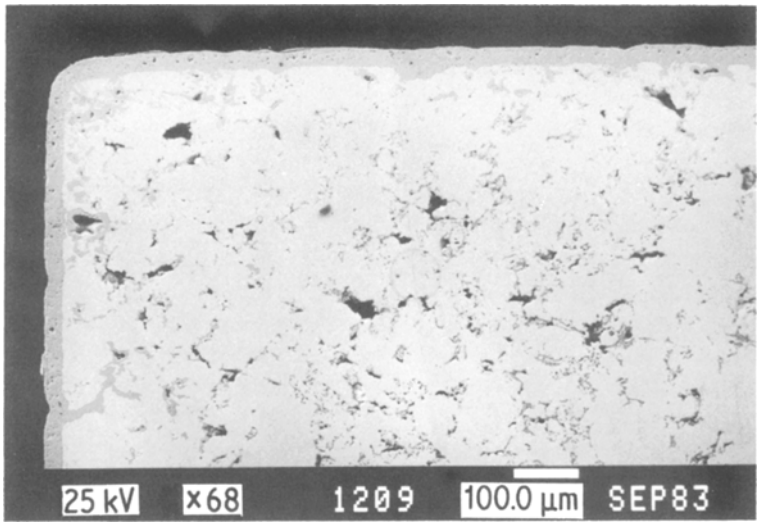

Figure 13 Cross-section of specimen soaked at 450° C for 7 days.

4. Conclusions

The normal creep laws for metals can be applied to sintered carbon steels up to 450° C. Primary creep can be described by a power law. Even at comparatively low stresses the dependence of the secondary creep rate on stress is best described by the exponential law. The temperature dependence of the secondary creep rate can be expressed in terms of a creep activation energy which is identifiable with the self diffusion activation energy even though the temperatures are well below $0.5\,T_m$. Because the creep-rupture time is inversely proportional to the secondary creep rate, the OSD parameter can be used to construct a master rupture curve. Over the range of stress and temperature used in these experiments the creep-rupture strength is a linear function of $[\ln t_R - (\Delta H_c/RT)]$. A master curve can be constructed equally well using the LM parameter. Although at present we cannot definitely prove that the OSD parameter is more correct we do feel that the present data tend to favour it.

We have used the OSD parameter to predict the mean rupture strengths of the 0.77% carbon sintered steel given in Table II. For design purposes the rupture strength that 95% of specimens can be assumed to achieve is about 20 MPa lower than the mean strength. These rupture strengths are a much smaller percentage of the room temperature tensile strength than comparative values for rolled carbon steel plate (see Table III). All sintered metals are likely to have similar low rupture strengths because the pores can start to grow in size immediately on loading without any prior creep to form voids. Since the creep-rupture strength depends on the strain $(\varepsilon_R - \varepsilon_1)$ one would expect that sintered metals with as large a ductility as possible would give the best rupture to ultimate strength ratios.

The surface oxidation rate for sintered steels is considerably greater than that of comparable conventional steels. Internal oxidation, however, is slight because the interconnecting pore system

TABLE II Creep-rupture strengths in (MPa expressed as a percentage of the UTS in brackets) of a 0.77% carbon 2% copper sintered steel of density 6800 kg m^{-3} estimated from Fig. 10

Temperature (° C)	Rupture time (h)			
	100	1000	10 000	100 000
250	370 (0.92)	330 (0.82)	290 (0.72)	250 (0.61)
350	220 (0.53)	170 (0.43)	130 (0.33)	90 (0.22)
450	100 (0.26)	60 (0.15)	20 (0.05)	– –

TABLE III Average creep-rupture strengths in (MPa expressed as a percentage of the UTS in brackets) for carbon manganese steel (0.13–0.2% C, 1.02–1.54% Mn)

Temperature (° C)	Rupture time (h)			
	100	1000	10 000	100 000
400	330 (0.70)	280 (0.59)	200 (0.42)	150 (0.32)
450	240 (0.51)	180 (0.38)	130 (0.28)	80 (0.17)

soon becomes blocked by the oxidation. The oxidation causes a slight reduction in the tensile strength of sintered steel due simply to the reduction in the cross-sectional area.

Acknowledgements

The grant by the Sydney County Council that enabled the purchase of the creep testing system is gratefully acknowledged. The powders used to manufacture the specimens were donated by Australian National Industries Ltd who also allowed the use of their sintering furnace for which we thank them.

References

1. F. GAROFALO, "Fundamentals of Creep and Creep-Rupture in Metals" (Macmillan, New York, 1965) pp. 15–16, 62–64.
2. H. W. MEAD and C. E. BIRCHENALL, *Trans. AIME* **206** (1956) 1336.
3. R. L. ORR, O. D. SHERBY and J. E. DORN, *Trans. ASM* **46** (1954) 113.
4. F. GAROFALO, R. W. WHITMORE, W. F. DOMIS and F. VON GEMMINGEN, *Trans. AIME* **221** (1961) 430.
5. H. J. TAPSELL, "Creep of Metals" (Oxford University Press, London, 1931) pp. 132–33.
6. F. R. LARSON and J. MILLER, *Trans. ASME* **74** (1952) 765.
7. P. FRANKLIN and B. L. DAVIES, *Powder Metall.* **20** (1977) 11.
8. N. D. TOMASHOV, "Theory of Corrosion and Protection of Metals" (Macmillan, New York, 1966) pp. 80–86.

Received 18 December 1983
and accepted 10 April 1984